INTERNATIONAL JOURNAL FOR NUMERICAL METHODS IN FLUIDS
Int. J. Numer. Meth. Fluids 2002; **40**:197–207 (DOI: 10.1002/fld.338)

Numerical evaluation of two discontinuous Galerkin methods for the compressible Navier–Stokes equations

F. Bassi[1,†] and S. Rebay[2,*,‡]

[1] *Dipartimento di Energetica, Università di Ancona, Via Brecce Bianche, 60100 Ancona, Italy*
[2] *Diparimento di Ingegneria Meccanica, Università di Brescia, Via Branze 38, 25123 Brescia, Italy*

SUMMARY

This paper presents a critical comparison between two recently proposed discontinuous Galerkin methods for the space discretization of the viscous terms of the compressible Navier–Stokes equations. The robustness and accuracy of the two methods has been numerically evaluated by considering simple but well documented classical two-dimensional test cases, including the flow around the NACA0012 airfoil, the flow along a flat plate and the flow through a turbine nozzle. Copyright © 2002 John Wiley & Sons, Ltd.

1. INTRODUCTION

The discontinuous Galerkin (DG) method is a recently developed higher-order accurate method which has been receiving great attention by several research groups. DG methods are in fact particulary well suited for the construction of high-order accurate space discretization of advective problems on general unstructured grids since they combine two features which usually appear separately in classical (continuous) finite element (FE) methods and in upwind finite volume (FV) methods. High-order accuracy is in fact pursued by means of high-order polynomial approximations within elements similarly to classical FE methods, and, at the same time, the physics of wave propagation is accounted for by Riemann solvers as in upwind FV methods. Additional advantages of DG discretization are compactness (coupling being restricted to the elements sharing a face) and the possibility to accomodate elements of varying order of accuracy within the same grid without difficulty, thus opening the way to a straightforward implementation of h–p adaptive methods.

In the last few years the DG method, originally conceived for purely advective problems, has been extended to treat advection–diffusion problems and has proved very successful in the numerical solution of the Navier–Stokes (NS) equations. Several schemes for the discretization of the viscous terms have been proposed in the literature, such as, among the many available,

*Correspondence to: S. Rebay, Dipartimento di Ingegneria Meccanica, Università di Brescia, Via Branze 38, 25123 Brescia, Italy.
† E-mail: f.bassi@popsci.unian.it
‡ E-mail: rebay@ing.unibs.it

Received May 2001
Revised October 2001

those developed by the authors [1–3], the local DG method of Cockburn and Shu [4], the method developed by Baumann and Oden (BO) [5–7] and the stabilized version of the BO method (called NIPG) recently analysed in Reference [8]. See also References [9, 10] for a general account of DG methods for purely elliptic problems.

The aim of this paper is to present a critical comparison between two of the previously mentioned methods, namely that introduced by the authors, see e.g. References [2, 3] and the method of Baumann and Oden described in References [5, 6]. These two methods, hereafter referred to as BR and BO, respectively, have in fact similar formulations and the BO method might be regarded as a cheaper alternative to the more involved BR method (see the next section).

The BR and BO schemes have been implemented in an implicit code which uses the preconditioned GMRES iterative linear system solver with the incomplete LU factorization preconditioner. Their robustness and accuracy has been evaluated by considering simple purely diffusive linear two-dimensional (2D) problems and the compressible 2D NS equations. In the latter case, which is the only one here reported for reasons of brevity, several flow conditions have been computed, including the flow around a NACA0012 profile for two different flow conditions, the laminar flow over a flat plate, and the 2D subsonic flow through a turbine nozzle.

2. DISCONTINUOUS GALERKIN SCHEMES FOR THE NS EQUATIONS

The compressible NS equations can be written in compact form as

$$\frac{\partial u}{\partial t} + \boldsymbol{\nabla} \cdot \mathbf{f}_{\mathrm{c}}(u) + \boldsymbol{\nabla} \cdot \mathbf{f}_{\mathrm{v}}(u, \boldsymbol{\nabla} u) = 0$$

where $u \in \mathbb{R}^{d+2}$ is the vector of the conservative variables, $\mathbf{f}_{\mathrm{c}}(u)$ and $\mathbf{f}_{\mathrm{v}}(u, \boldsymbol{\nabla} u) = \mathscr{A}_{\mathrm{v}}(u) \boldsymbol{\nabla} u \in \mathbb{R}^{d+2} \otimes \mathbb{R}^{d}$ are the inviscid and viscous flux functions, respectively, d denoting the number of space dimensions. The weak formulation of the NS equations can be written as

$$\sum_{e} \left[\int_{\Omega_e} \phi \frac{\partial u}{\partial t} \, \mathrm{d}\Omega + \oint_{\partial \Omega_e} \phi \mathbf{n} \cdot \mathbf{f}(u, \boldsymbol{\nabla} u) \, \mathrm{d}\sigma - \int_{\Omega_e} \boldsymbol{\nabla} \phi \cdot \mathbf{f}(u, \boldsymbol{\nabla} u) \, \mathrm{d}\Omega \right] = 0, \quad \forall \phi \tag{1}$$

in which $\mathbf{f}(u, \boldsymbol{\nabla} u) = \mathbf{f}_{\mathrm{c}}(u) + \mathbf{f}_{\mathrm{v}}(u, \boldsymbol{\nabla} u)$, and the integral over the domain Ω has been split into the sum of integrals over the elements e before integration by parts.

To put in evidence the different role played by the contour integral for internal interfaces and for boundary sides, the second summation appearing in Equation (1) can be rearranged as a sum over internal interface integrals plus a sum over boundary side integrals. If Γ denotes the union of internal interface sides and Σ the union of boundary sides, Equation (1) can be rewritten as

$$\begin{aligned} &\int_{\Omega} \phi \frac{\partial u}{\partial t} \, \mathrm{d}\Omega - \int_{\Omega} \boldsymbol{\nabla} \phi \cdot \mathbf{f}(u, \boldsymbol{\nabla} u) \, \mathrm{d}\Omega \\ &\quad + \int_{\Gamma} [\phi^{-} \mathbf{n}^{-} \cdot \mathbf{f}(u^{-}, \boldsymbol{\nabla} u^{-}) + \phi^{+} \mathbf{n}^{+} \cdot \mathbf{f}(u^{+}, \boldsymbol{\nabla} u^{+})] \, \mathrm{d}\sigma \\ &\quad + \int_{\Sigma} \phi \mathbf{n}^{-} \cdot \mathbf{f}(u^{*}, \boldsymbol{\nabla} u^{*}) \, \mathrm{d}\sigma, \quad \forall \phi \end{aligned} \tag{2}$$

The notation $(\cdot)^-$ and $(\cdot)^+$ denotes the interface value of any quantity associated to the two elements sharing a face, and the normal unit vector $\mathbf{n}^-$ points outward from the element associated to the values $(\cdot)^-$, and $\mathbf{n}^- + \mathbf{n}^+ = \mathbf{0}$.

The flux function arguments u^* and ∇u^* appearing in the boundary integral are introduced in order to prescribe the boundary conditions, and are given by

$$u^* = u^{\mathrm{b}}, \quad \nabla u^* = \nabla u^-$$

to prescribe Dirichlet conditions, and by

$$u^* = u^-, \quad \mathbf{n} \cdot \nabla u^* = \mathbf{n} \cdot \nabla u^{\mathrm{b}}, \quad \mathbf{n}^\perp \cdot \nabla u^* = \mathbf{n}^\perp \cdot \nabla u^-$$

to prescribe Neumann conditions. The value of u^{b} for inflow, outflow and farfield boundaries is computed using a characteristic analysis in the direction $\mathbf{n}$ whereby the state u^{b} is obtained by combining the information associated to the outgoing characteristics computed with the internal state u^- and the prescribed boundary data.

Due to the discontinuous approximation adopted for ϕ and u, the interface integral term appearing in Equation (2) does not disappear as in standard continuous finite element methods. It is therefore necessary to resort to an interface flux treatment in order to guarantee conservation and to provide the coupling between neighbouring elements which would be otherwise completely missing.

For the inviscid NS (Euler) equations, this is in general accomplished by replacing the physical normal flux $\mathbf{n} \cdot \mathbf{f}_{\mathrm{c}}(u)$ with a numerical flux $h(u^-, u^+; \mathbf{n}^-)$ analogous to that commonly employed in upwind finite volume methods. In our computations we have used the van Leer flux difference splitting numerical flux as modified by Hänel.

An interface treatment for the viscous part of the NS is instead not readily available from FV methods. In previews works the authors have introduced two DG schemes for the NS viscous terms that rely upon the definition of interface functions $\delta^{\pm}$ accounting for interface variable jumps (see e.g. References [11, 2]) or interface viscous flux jumps [3]. We here consider the latter scheme which can be written in semi-discrete form as

$$\begin{aligned}
&\int_\Omega \phi \frac{\partial u}{\partial t} \,\mathrm{d}\Omega - \int_\Omega \nabla\phi \cdot \mathbf{f}(u, \nabla u) \,\mathrm{d}\Omega \\
&\quad + \int_\Gamma (\phi^- h^- + \phi^+ h^+) \,\mathrm{d}\sigma + \frac{1}{2} \int_\Gamma [(\nabla\phi^{\mathrm{T}} \mathscr{A}_{\mathrm{v}} \mathbf{n})^+ - (\nabla\phi^{\mathrm{T}} \mathscr{A}_{\mathrm{v}} \mathbf{n})^-](u^+ - u^-) \,\mathrm{d}\sigma \\
&\quad + \frac{1}{2} \int_\Gamma (\phi^+ - \phi^-)[(\mathbf{n}^{\mathrm{T}} \mathscr{A}_{\mathrm{v}} \nabla u)^+ - (\mathbf{n}^{\mathrm{T}} \mathscr{A}_{\mathrm{v}} \nabla u)^-] \,\mathrm{d}\sigma + \frac{1}{2} \int_\Gamma (\phi^+ - \phi^-)(\delta_n^+ - \delta_n^-) \,\mathrm{d}\sigma \\
&\quad + \int_\Sigma \phi \mathbf{n} \cdot \mathbf{f}_{\mathrm{c}}(u^{\mathrm{b}}) \,\mathrm{d}\sigma - \int_\Sigma (\nabla\phi^{\mathrm{T}} \mathscr{A}_{\mathrm{v}} \mathbf{n})^- (u^{\mathrm{b}} - u^-) \,\mathrm{d}\sigma \\
&\quad + \int_\Sigma \phi (\mathbf{n}^{\mathrm{T}} \mathscr{A}_{\mathrm{v}} \nabla u)^{\mathrm{b}}] \,\mathrm{d}\sigma + \int_\Sigma \phi \delta_n^{\mathrm{b}} \,\mathrm{d}\sigma = 0, \quad \forall\phi
\end{aligned} \tag{3}$$

The auxiliary variables $\delta_n^{\pm}$ appearing in the interface integral of Equation (3) are defined for each interface side as

$$\int_{\Omega_e^{\pm}} \phi^{\pm}\delta_n^{\pm}\,\mathrm{d}\Omega = -\frac{1}{2}\int_{\sigma_f} \phi^{\pm}(\mathbf{n}^{\mathrm{T}}\mathscr{A}_{\mathrm{v}}\mathbf{n})^{\pm}(u^{\mp}-u^{\pm})\,\mathrm{d}\sigma \tag{4}$$

while the variable δ_n^{b} appearing in the boundary integral is defined for each boundary side as

$$\int_{\Omega_e^{-}} \phi^{-}\delta_n^{\mathrm{b}}\,\mathrm{d}\Omega = \int_{\sigma_b} \phi^{-}(\mathbf{n}^{\mathrm{T}}\mathscr{A}_{\mathrm{v}}\mathbf{n})^{\mathrm{b}}(u^{\mathrm{b}}-u^{-})\,\mathrm{d}\sigma \tag{5}$$

The auxiliary variables δ_n can be therefore computed locally for each internal interface or boundary side in terms of $u^{\pm}$. The expansion coefficients δ_i of the function $\delta_n(\mathbf{x}) = \sum_i \delta_i N_i(\mathbf{x})$ are in fact related to the expansion coefficients $u_i^{\pm}$ of the function $u^{\pm}(\mathbf{x}) = \sum_i u_i^{\pm} N_i(\mathbf{x})$ by the expressions

$$\delta_i^{\pm} = (M_{ik}^{\pm})^{-1}K_{kj}^{\pm}(u_j^{\pm}-u_j^{\pm}), \quad \delta_i^{\mathrm{b}} = (M_{ik}^{-})^{-1}K_{kj}^{-}(u_j^{-}-u_j^{\mathrm{b}}) \tag{6}$$

in which the matrices $M^{\pm}$ and $K^{\pm}$ are given by

$$M_{ij}^{\pm} = \int_{\Omega_e^{\pm}} \phi_i^{\pm}\phi_j^{\pm}\,\mathrm{d}\Omega, \quad K_{ij}^{\pm} = \frac{1}{2}\int_{\sigma_f} [\phi_i(\mathbf{n}^{\mathrm{T}}\mathscr{A}_{\mathrm{v}}\mathbf{n})\phi_j]^{\pm}\,\mathrm{d}\sigma$$

Scheme (3), with the function δ_n expressed in terms of the function $u^{\pm}$ according to Equation (4) or (5), provides a DG space discretization of the NS equations entirely in terms of the original variable u. The scheme is characterized by a very compact support since the unknowns associated with an element e are only coupled with the unknowns associated with the elements which share a face with e. This results in a discretized spatial operator which can be solved very efficiently and is therefore very well suited to be used with an implicit time-integration scheme.

The second DG method for the NS equation here considered is that introduced by Baumann and Oden (see e.g. References [5, 6]), which bears some resemblance with the BR scheme and in fact can be obtained from Equation (3) by removing the interface and boundary integral terms involving the auxiliary variables δ_n and by changing the sign of the third interface and a boundary integrals. The BO scheme in semi-discrete form can therefore be written as

$$\begin{aligned}
&\int_{\Omega} \phi\frac{\partial u}{\partial t}\,\mathrm{d}\Omega - \int_{\Omega} \nabla\phi\cdot\mathbf{f}(u,\nabla u)\,\mathrm{d}\Omega \\
&\quad + \int_{\Gamma} (\phi^{-}h^{-}+\phi^{+}h^{+})\,\mathrm{d}\sigma + \frac{1}{2}\int_{\Gamma} [(\nabla\phi^{\mathrm{T}}\mathscr{A}_{\mathrm{v}}\mathbf{n})^{+} - (\nabla\phi^{\mathrm{T}}\mathscr{A}_{\mathrm{v}}\mathbf{n})^{-}](u^{+}-u^{-})\,\mathrm{d}\sigma \\
&\quad - \frac{1}{2}\int_{\Gamma} (\phi^{+}-\phi^{-})[(\mathbf{n}^{\mathrm{T}}\mathscr{A}_{\mathrm{v}}\nabla u)^{+} - (\mathbf{n}^{\mathrm{T}}\mathscr{A}_{\mathrm{v}}\nabla u)^{-}]\,\mathrm{d}\sigma \\
&\quad + \int_{\Sigma} \phi\mathbf{n}\cdot\mathbf{f}_{\mathrm{c}}(u^{\mathrm{b}})\,\mathrm{d}\sigma - \int_{\Sigma} (\nabla\phi^{\mathrm{T}}\mathscr{A}_{\mathrm{v}}\mathbf{n})^{-}(u^{\mathrm{b}}-u^{-})\,\mathrm{d}\sigma \\
&\quad - \int_{\Sigma} \phi(\mathbf{n}^{\mathrm{T}}\mathscr{A}_{\mathrm{v}}\nabla u)^{\mathrm{b}}]\,\mathrm{d}\sigma = 0, \quad \forall\phi
\end{aligned} \tag{7}$$

The BO scheme is simpler than the BR scheme because of the lack of the terms involving the auxiliary variable δ_n but, because of the change in signs, it leads to an unsymmetric discretization of the diffusion operator (even for a symmetric viscous Jacobian matrix $\mathcal{A}_v$). This is not at all a drawback if the method is used to solve an advection diffusion problem since the advection part of the problem is already intrinsically unsymmetric. There is however a small price to pay for the lack of the δ_n terms, in that the BO scheme, unlike BR scheme, cannot employ piecewise constant elements for viscous computations.

Schemes (3) and (7) are advanced in time with the implicit backward Euler time-integration scheme. The linearization of the NS equations is simply accomplished by evaluating all the Jacobians, both inviscid and viscous, at time level n, thus reducing both the inviscid and the viscous parts of the NS equations to linear operators in u. The linear systems arising at each time step are solved by means of the preconditioned GMRES iterative solution algorithm implemented in the SLAP package available in the Netlib public domain library. A reasonable compromise between efficiency and storage requirements has been found by using the incomplete LU factorization preconditioner.

3. NUMERICAL RESULTS

The accuracy of the BR and BO schemes has been evaluated by considering simple purely diffusive problems and the compressible NS equations. The results obtained for the purely diffusive test cases seem to indicate that the BR scheme is more robust and usually more accurate than the BO scheme. For example, unlike the BR scheme, the BO method cannot solve the Laplace equation on the unit square with P1 elements (but works with P2 or higher-order elements). For reason of space we will however concentrate on the results obtained for the NS computations.

The first test case considered is the transonic flow around a NACA0012 airfoil at an angle of attack $\alpha = 10°$, Reynold number $Re_\infty = 73$ and Mach number $M_\infty = 0.8$. This is commonly considered an easy test problem, but we have made it harder than usual by solving it on a rather coarse grid—the triangulation of a regular distribution of 64×16 points obtained by a conformal mapping method—in order to put in evidence possible differences of the two schemes.

Figures 1 and 2 show the Mach isolines computed with linear elements (P1) obtained with the BR and the BO schemes. The two P1 solutions look very similar, the BO being slightly more discontinuous than the BR one. This difference is more clearly displayed by Figures 3 and 4, which show an enlargement of the computed P1 Mach isolines near to the profile trailing edge. The different performance of the two schemes is much more evident when we consider quadratic (P2) elements. The BR scheme converged very easily to steady state, and the computed Mach isolines around the entire profile are shown in Figure 5. On the contrary we have not been able to compute a P2-BO solution at all. The BO scheme in fact diverges even when starting from the P2 converged solution obtained with the BR scheme. The divergence of the BO scheme is originated in the region near to the trailing edge, see Figure 6, which shows the P2-BO Mach isolines just before the computation failure. These results seem to indicate that, unlike the BR scheme, the BO interface flux treatment is not able to cope with the solution discontinuities if the grid is not sufficiently fine to allow an accurate representation of the solution.

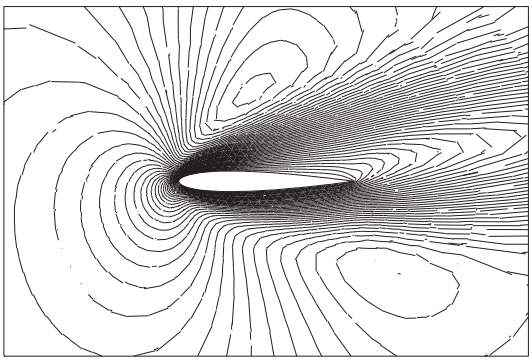

Figure 1. NACA0012 global view, $Re = 73$ Mach isolines, P1 elements, BR scheme.

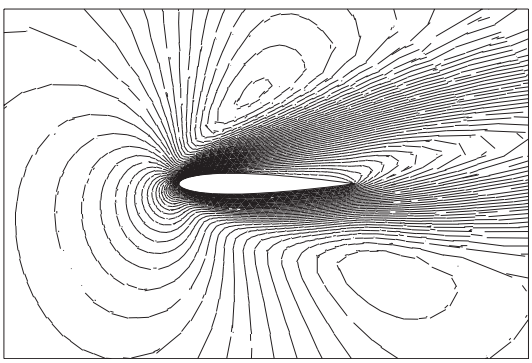

Figure 2. NACA0012 global view, $Re = 73$ Mach isolines, P1 elements, BO scheme.

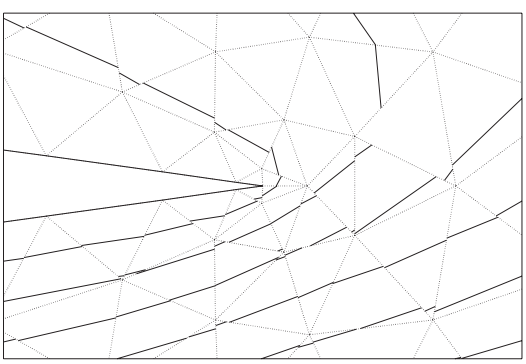

Figure 3. NACA0012 trailing edge, $Re = 73$ Mach isolines, P1 elements, BR scheme.

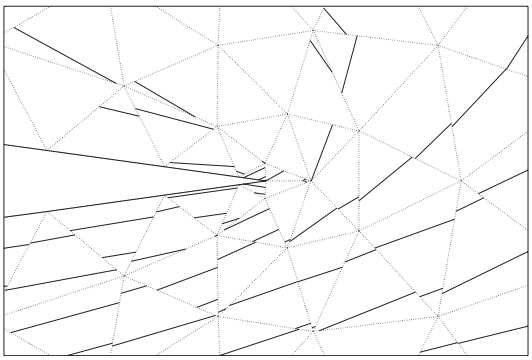

Figure 4. NACA0012 trailing edge, $Re = 73$ Mach isolines, P1 elements, BO scheme.

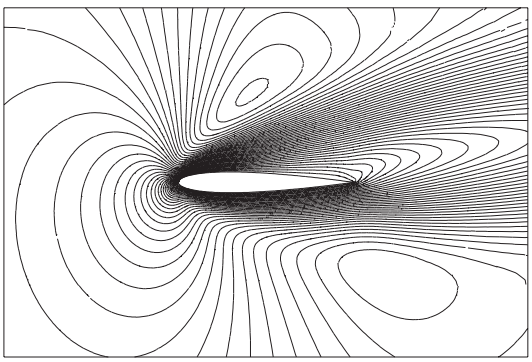

Figure 5. NACA0012 global view, $Re = 73$ Mach isolines, P2 elements, BR scheme.

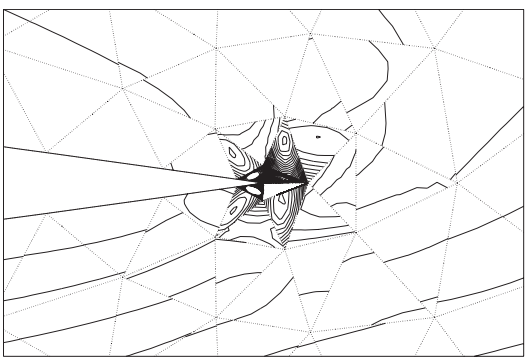

Figure 6. NACA0012 trailing edge, $Re = 73$ Mach isolines, P2 elements, BO scheme.

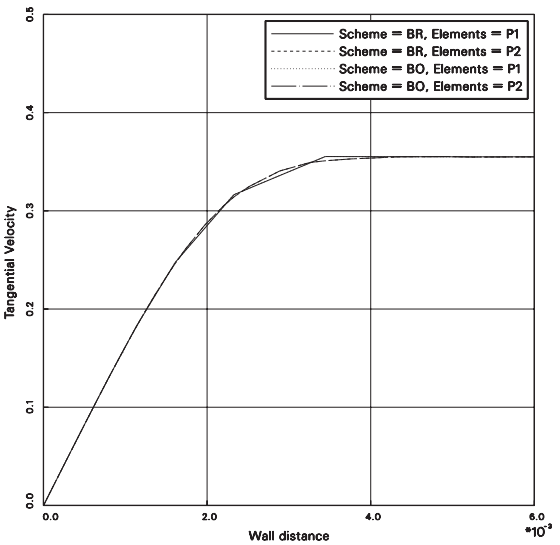

Figure 7. Flat plae, $Re = 10^6$, velocity profiles tangential to the wall.

The different behaviour of the two schemes is more evident in the second test case—the computation of the subsonic flow around a NACA0012 airfoil at an angle of attack $\alpha = 0°$, Reynold number $Re_\infty = 5000$ and Mach number $M_\infty = 0.5$. The difficulties related to a grid which is not sufficiently fine to accurately resolve the solution are here more serious since we have used the same grid of the previous test case for a higher Reynolds number computation. In fact the BR scheme performs very well on this problem (see e.g. Reference [3]), while we have not been able to obtain P1-BO or P2-BO solutions at all, even when using as initial data the corresponding converged solution computed with the BR scheme.

The third case consists in the calculation of the laminar flow over a flat plate for a Reynolds number $Re_\infty = 10^6$ and Mach number $M_\infty = 0.3$. In this case we have used a stretched grid—containing 1600 triangles and 867 points—in order to verify the behaviour of the BO scheme in a problem where, despite the very high Reynolds number value, the grid is sufficiently fine to accurately resolve the flow field. Figures 7 and 8 [t] show the very good agreement between the computed velocity profiles at the plate mid-length obtained with P1/P2-BR/BO schemes. The results therefore seem to indicate that, for sufficiently refined grids, the BR and the BO schemes give quite similar results.

We have finally performed test computations of the subsonic flow through a turbine nozzle for an inlet angle $\alpha_1 = 0°$, Reynolds number $Re = 0.966 \times 10^6$ and $M_{is} = 0.68$ (M_{is} denotes the 'isentropic Mach number', a parameter commonly employed in the turbomachinery literature to express the outlet pressure of turbine nozzles). The purpose of this test case is to check the two methods for a complex high Reynolds number flow of turbomachinery interest using a stretched grid which is sufficiently fine to accurately resolve the flow field and which should therefore be adequate for both the BR and the BO schemes as in the flat plate test case. The BR and BO schemes performed in fact equally well for this test case, at least if P1

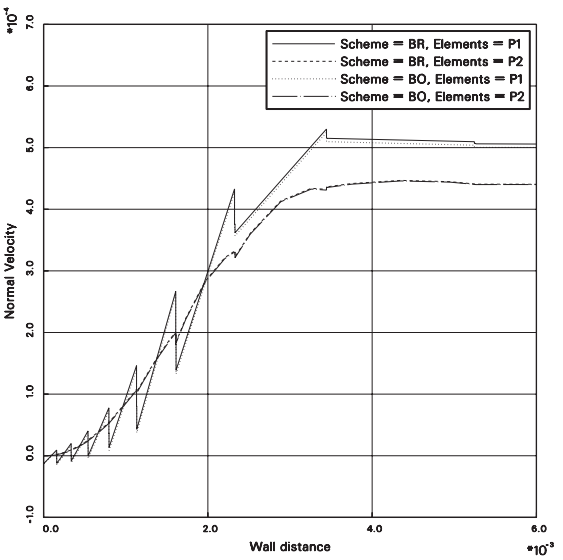

Figure 8. Flat plate, $Re = 10^5$, velocity profiles normal to the wall.

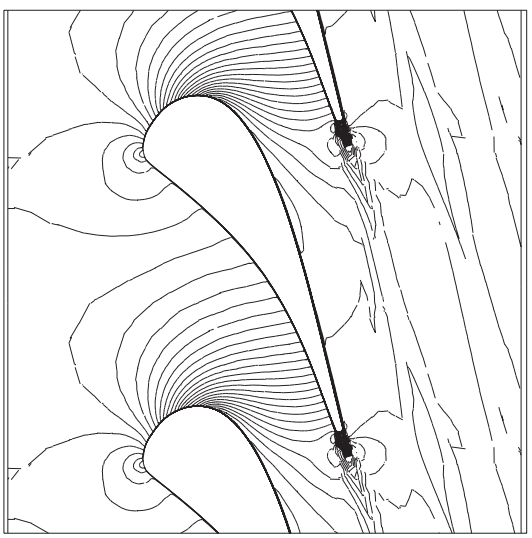

Figure 9. LS89, $Re = 966000$, Mach isolines, P1 elements, BR scheme.

elements are used (we have not attempted the more expensive P2 computation for reasons of time, but we expect that both method should give similar solutions also for P2 elements). Figures 9 and 10 show the Mach isolines computed with the BR and BO schemes, and the solutions look very similar indeed. These results are a further confirmation that, provided that

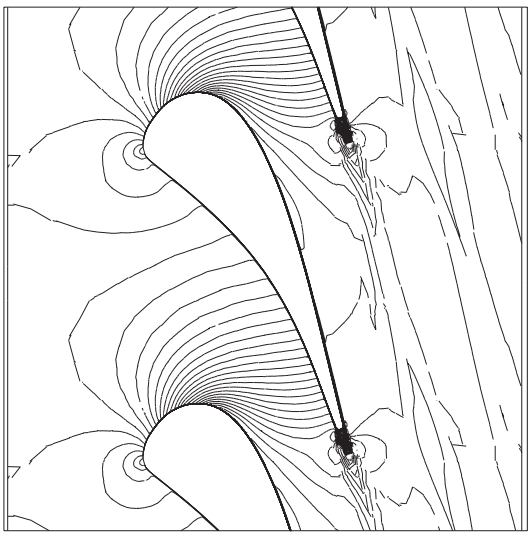

Figure 10. LS89, $Re = 966000$, Mach isolines, P1 elements, BO scheme.

the grids are sufficiently fine to accurately resolve the solution features, both the BR and the BO schemes have a very similar performance.

4. CONCLUSIONS

Two recently developed DG methods for the numerical solution of the compressible NS equations have been described and compared by solving 2D test cases ranging from simple airfoil computations at very low Reynolds number to the simulation of the subsonic high Reynolds number flow through a turbine nozzle.

Our test computations reveal that the performance of the two method is very similar provided that the grid is sufficiently fine to accurately resolve the solution. On the contrary, the performance of the two methods seems quite different if the grid is coarse and the numerical solution displays significant discontinuities at the element interfaces. In this case, as shown by the NACA0012 computations, the BR scheme is still able to compute reasonable solutions when the BO scheme does not. This behaviour needs further analysis in view of the expected performance of DG methods on relatively coarse and/or strongly non-uniform grids.

REFERENCES

1. Bassi F, Rebay S. A high-order accurate discontinuous finite element method for the numerical solution of the compressible Navier–Stokes equations. *Journal of Computational Physics* 1997; **131**:267–279.
2. Bassi F, Rebay S. An implicit high-order discontinuous Galerkin method for the steady state compressible Navier–Stokes equations. In *Computational Fluid Dynamics 98*, *Proceedings of the Fourth European Computational Fluid Dynamics Conference*, Papailiou KD, Tsahalis D, Périaux J, Hirsh C, Pandolfi M (eds). Wiley: New York, 1998; 1227–1233.

3. Bassi F, Rebay S. GMRES discontinuous Galerkin solution of the compressible Navier–Stokes equations. In *Discontinuous Galerkin methods*: *Theory*, *Computation and Applications*, Cockburn B, Karniadakis GE, Shu C-W (eds). Springer: Berlin, 2000; 197–208.
4. Cockburn B, Shu C-W. The local discontinuous Galerkin finite element method for convection–diffusion systems. *SIAM Journal of Numerical Analysis* 1998; **175**:2440–2463.
5. Baumann CE, Oden JT. A discontinuous hp finite element method for convection–diffusion problems. *Computational Methods in Applied Mechanical Engineering* 1999; **175**:311–341.
6. Baumann CE, Oden JT. A discontinuous hp finite element method for the Euler and Navier–Stokes equations. *International Journal for Numerical Methods in Fluids* 1999; **31**:79–96.
7. Oden JT, Babuska I, Baumann CE. A discontinuous hp finite element method for diffusion problems. *Journal of Computational Physics* 1998; **146**:491–519.
8. Riviere B, Wheeler MF, Girault V. Improved energy estimates for interior penalty, constrained and discontinuous Galerkin methods for elliptic problems. Part I, *Technical Report 3 Computational Geosciences*, 1999.
9. Arnold D, Brezzi F, Cockburn B, Marini D. Discontinuous Galerkin methods for elliptic problems. In *Discontinuous Galerkin methods*: *Theory*, *Computation and Applications*, Cockburn B, Karniadakis GE, Shu C-W (eds). Springer: Berlin, 2000; 89–101.
10. Arnold D, Brezzi F, Cockburn B, Marini D. Unified analysis of discontinuous Galerkin methods for elliptic problems. *SIAM Journal of Numerical Analysis* 2002 at press.
11. Bassi F, Rebay S, Mariotti G, Pedinotti S, Savini M. A high-order accurate discontinuous finite element method for inviscid and viscous turbomachinery flows. In *Second European Conference on Turbomachinery Fluid Dynamics and Thermodynamics*, Decuypere R, Dibelius G (eds). Technologisch Instituut: Antwerp, 1997; 99–108.

